Pressure-induced crystalline to amorphous transition in hydroxylapatite

S. N. VAIDYA, C. KARUNAKARAN, B. M. PANDE, N. M. GUPTA
Chemistry Division, Bhabha Atomic Research Centre, Trombay, Bombay 400 085, India
R. K. IYER, S. B. KARWEER
Applied Chemistry Division, Bhabha Atomic Research Centre, Bombay 400 085, India

Hydroxylapatite, prepared by the reaction of an aqueous suspension of $Ca(OH)_2$ with H_3PO_4 at pH >7 and sintered at 700 °C was subjected to various pressures in a Bridgman anvil apparatus, and the retrieved material was examined by X-ray diffraction (XRD), Fourier transform infrared spectroscopy (FTIR) and scanning electron microscopy (SEM) methods. The studies showed that the crystalline hydroxylapatite transforms irreversibly to an amorphous phase 2 GPa. The transformation occurs through an intermediate phase and is completed at around 10 GPa pressure.

1. Introduction

In recent years considerable attention has been paid to hydroxylapatite (HA), $Ca_5(PO_4)_3(OH)$, which is the primary constituent of human bones and teeth and is a potential biomaterial for the bone and tooth implants [1–4]. Many studies have been reported on synthesis, crystallographic properties, thermal stability [5–10] and infrared and Raman spectra [11, 12] of HA prepared by different methods. The flexural and the compressive strengths of HA ceramics have been studied for the dental and orthopedic purposes. Naturally, occurring apatite has also been a subject of mineralogical studies [11, 13–15]. However, there are no studies, to our knowledge, on the effect of pressure on crystalline HA. In this paper we report first observation of the pressure-induced transformation in HA from a crystalline form to an amorphous (c → a) state, which is completed at about 10 GPa.

2. Experimental procedure

2.1. Preparation

HA is prepared by a slow and a dropwise addition of dilute H_3PO_4 (0.3 mol H_3PO_4 in 1 l water) to a constantly stirred aqueous suspension of $Ca(OH)_2$ (0.5 mol in 1 l water) in molar ratio 3:5 while maintaining pH >7. Our preliminary experiments showed that Ca/P ratio in the product was less than 1.67 if the final pH was less than 7. Hence, the experimental conditions were modified to ensure that pH remained more than 7 during preparation. This was achieved by addition of a small quantity of dilute NaOH solution towards the end of the reaction when the pH tends to drop below 7. After precipitation, the reaction mixture was stirred for 1 h and aged at room temperature for 10 days. The slurry was filtered and washed twice with distilled water. The cake thus formed was dried at 80 °C. It was then powdered, heated again to 80 °C before sintering at 700 °C for 6 h. The Ca content in HA was determined volumetrically by titration with permanganate solution after precipitation of Ca as CaC_2O_4, while the phosphate content was estimated gravimetrically as $Mg_2P_2O_7$. The sodium content was determined by atomic absorption spectroscopy.

The synthesized material was characterized by X-ray diffraction (XRD) and Fourier transform infrared (FTIR) methods. The FTIR studies showed that the HA contained nearly 0.6 wt % CO_2 as carbonate. The infrared bands observed with our sample corresponded closely with the earlier reported data on the natural and the synthetic HA [11, 16]. The chemical composition of our HA, without considering the carbonate content, is $Ca_{9.92}Na_{0.048}(PO_4)_6(OH)_{1.89}$. The X-ray diffraction patterns were recorded with CuK_α radiation using a Philips PW 1820 wide-angle goniometer mounted on PW 1729 X-ray generator. The data were processed using a PW 1710 microprocessor coupled to a PC AT. The XRD pattern matched well with that reported for HA (space group $P6_3/m$) with $a = 0.943$ and $c = 0.688$ nm [17, 18]. FTIR spectroscopy studies were performed using a Mattson model Cygnus100 spectrometer equipped with a Deuterated Tryglicine Sulfate (DTGS) detector. For this purpose, thin wafers containing 5% of a sample in KBr were prepared and for each sample 50–100 scans were accumulated at 4 cm^{-1} resolution. All the spectra were recorded in transmittance mode with the air as reference.

High-pressure experiments employed Bridgman anvils having face diameter 12.7 mm and pyrophyllite gaskets 12.7 mm o.d. × 5.3 mm i.d. × 0.5 mm thick for experiments upto 8 GPa [19], and anvils having face diameter 6.3 mm and pyrophyllite gaskets 6.3 mm o.d. × 3 mm i.d. × 0.5 mm thick for the experiment at

0022–2461

10.5 GPa [20]. The anvils were calibrated by monitoring) the resistance discontinuity at the Bi (I–II and III–IV) and Fe (bcc → hcp) transition. The 0.45 mm thick compressed discs of HA were used as starting material. These discs were placed in the centre of pyrophyllite gasket and kept at a desired pressure for 72 h. The pressurized material thus obtained was retrieved and examined by XRD and FTIR techniques. The morphology of the specimens was studied using a Jeol 330A scanning electron microscope.

3. Results and discussion

3.1. XRD studies

Hydroxylapatite powder, which is white and translucent, transformed progressively to a nearly transparent material on being subjected to high pressures. Also, the XRD patterns of the HA specimens showed progressive transformation to amorphous phase, as indicated in the data of Fig. 1a–e. The XRD pattern of an unpelletized HA sample is given in Fig. 1a for reference, which is in conformity with the reported crystal structure of this material [17, 18]. The XRD pattern of HA pressed to 2.0 GPa shows four prominent lines at 0.287, 0.277, 0.228 and 0.196 nm. (Fig. 1b). These are the (2 1 1), (1 1 2), (2 1 2) and (2 2 2) diffraction lines. The d-spacings of these lines show a small increase over the normal values. Diffraction lines (0 0 2) and (0 0 4) are among those which are not observed in this pattern. Hence we infer that at around 2 GPa, the structure begins to collapse along the c-axis, while small expansion takes place in the a–b plane. This seems reasonable in view of the fact that the structural units in the hexagonal structure of HA [18, 21] are very loosely packed along the c-axis, as is discussed in a later section in detail. The increase in background intensity in the diffraction pattern of Fig. 1b at $d > 0.3$ nm ($2\theta < 30^\circ$) also signals the onset of amorphization on large length scale. At a pressure of 4.3 GPa, most of the diffraction lines disappear and a broad hump, characteristic of the amorphous phase, appears between $2\theta = 15^\circ$–35° (0.88–0.3 nm) (Fig. 1c). New diffraction lines are also seen at 0.228 and 0.218 nm in Fig. 1c. We attribute these reflections to the appearance of an unidentified precursor phase which vanishes with the further increase in pressure (Fig. 1d, e). However, the diffraction lines (2 1 1) at 0.281 nm and (1 1 2) at 0.275 nm at 1×10^5 Pa are seen even in the samples pressurized to 8.5 and 10.5 GPa (Fig. 1d, e). These observations thus clearly reveal the formation of an intermediate phase in HA at a pressure of about 4.3 GPa. With the increase in pressure, this intermediate phase disappears giving way to an amorphous phase. Appearance of such a precursor phase prior to amorphisation has been reported in α-SiO_2 [22]. The crystalline-to-amorphous transformation in HA reported above is found to be irreversible.

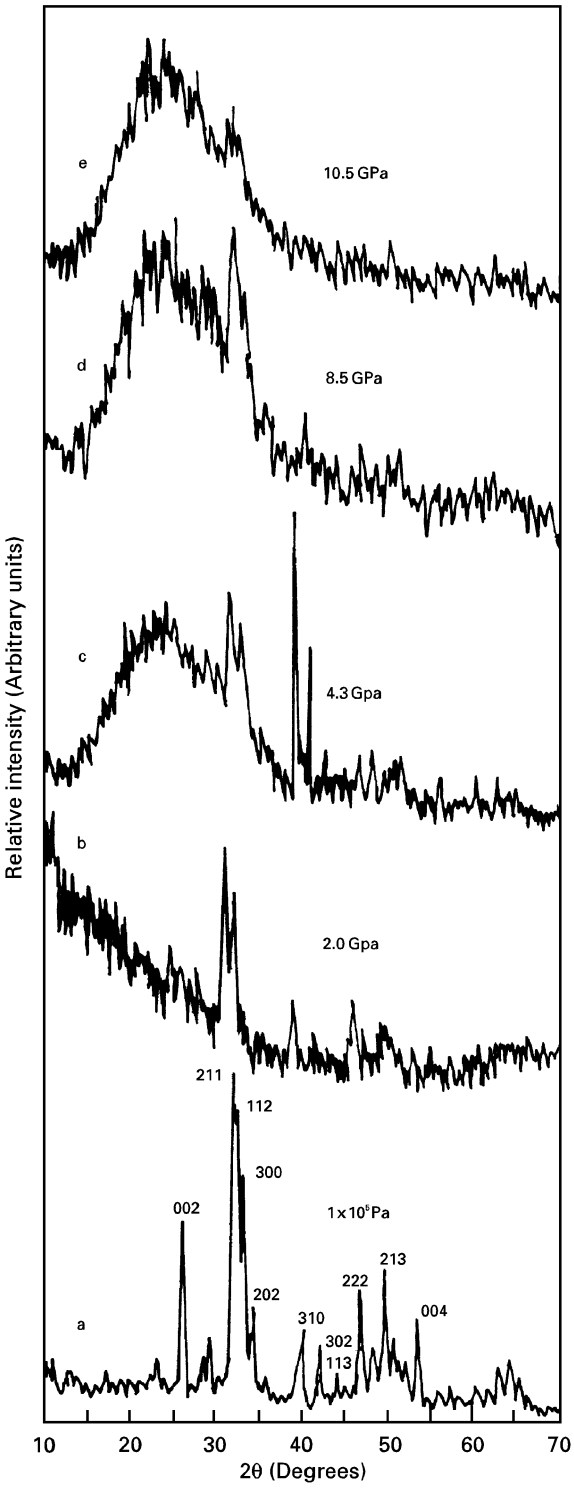

Figure 1 XRD patterns of hydroxylapatite as a function of applied pressure.

3.2. SEM studies

Fig. 2a shows the scanning electron micrograph of a HA disc pressed at 4.3 GPa. This micrograph exhibits regions of three distinct morphologies. The area marked "A" is relatively smooth while the region "C" is coarse. The intermediate region (I) has bright contrast. Region C is seen at a higher magnification in Fig. 2b. The crystallite size here varies from nearly 2 to 10 μm. At the same magnification no crystallites were seen in region A. The pellets subjected to higher pressures of 8.5 GPa were also examined by SEM and the micrographs revealed the presence of the regions similar to the areas marked as A and C in Fig. 2. No features similar to region I in Fig. 2 were, however, seen in this case.

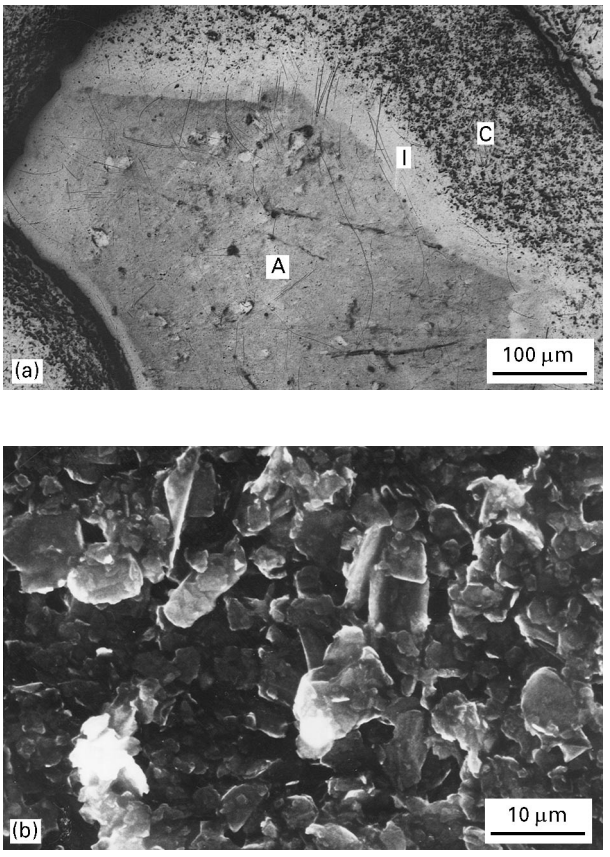

Figure 2 SEM Micrographs of a HA disc pressed to 4.3 GPa. (a) The micrograph shows the crystalline (C), amorphous (A) and intermediate (I) phases (× 100); (b) an enlarged view of crystalline phase (× 2000).

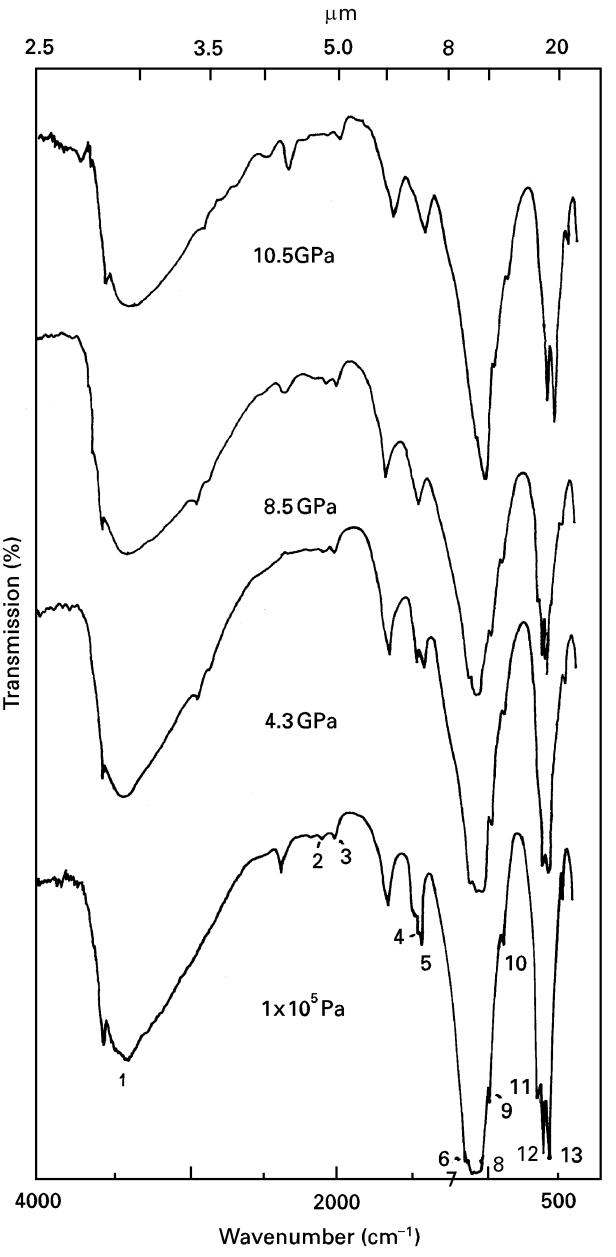

Figure 3 Effect of pressure of the FTIR spectrum of a HA disc.

3.3. FTIR studies

The application of pressure manifests in two ways in the infrared spectrum of HA. First, the transmittance of the sample wafer in the i.r. region of 400–4000 cm^{-1} increased progressively with the increasing pressure. Thus, the HA wafers showed a transmittance of 50, 60 and 75%, when the samples were subjected to a pressure of 4.2, 8.5 and 10.4 GPa, respectively. On the other hand, the compacted powder disc without application of high pressure showed a transmittance of $\sim$40%. Second, even though the frequency of all the i.r. bands remained unaffected within $+2\,cm^{-1}$, the width of the vibrational bands associated with the phosphate groups was reduced selectively with the increasing pressure.

The FTIR spectra of the unpressurized and the pressurized discs of HA are shown in Fig. 3 and the assignment of various absorption bands is given in Table I. The absorption frequencies reported recently for natural as well as synthetic HA [10, 11] are also given in the table. As discussed in reference 11, the i.r. absorption spectrum of HA is characterized by three main regions which are related to the vibrational frequencies of the OH^-, PO_4^{3-} and CO_3^{2-} ions. The absorption due to the internal stretching of OH is located at 3400 cm^{-1} and due to its libration at 630 cm^{-1}. A sharp and weak band at $\sim$3571 cm^{-1} in the spectra of Fig. 3 indicates the presence of some isolated hydroxyl groups, the nature of which cannot be ascertained now. The frequencies associated with the vibration of the phosphate ion are a symmetric stretch (ν_1), a doubly degenerate symmetric bend (ν_2) a triply degenerate asymmetric stretch (ν_3) and a triply degenerate asymmetric bend (ν_4) [11]. We observe all these modes except ν_2 mode which lies below 350 cm^{-1}. Also observed are the second harmonics of ν_3 between 2000 and 2150 cm^{-1}. The CO_3^{2-} has bands at 864, 1430 and 1455 cm^{-1} when carbonate ion replaces the phosphate ion [24, 25] and at 883, 1465 and 1542 cm^{-1} when it replaces the hydroxyl ion in HA. We have observed the absorption bands at 875, 1422 and 1455 cm^{-1}. This suggests that a small amount of carbonate gets incorporated during preparation and these carbonate ions mostly replace the phosphate ions in the HA lattice. Santos and Clayton [11] have experimentally determined correlation between the amount of carbonate in HA and the ratio of the areas of the carbonate and phosphate peaks in the i.r.

TABLE I Vibration frequencies (cm^{-1}) of hydroxylapatite (HA). Numbers in parentheses refer to the absorption peaks in Fig. 3.

Sample	ν_{OH} (vib)	PO_4 overtone, 2 ν_3	CO_3 asymmetric stretch	PO_4 asymmetric stretch ν_3	PO_4 symmetric stretch ν_4	CO_3	ν_{OH} (lib)	PO_4 asymmetric bend ν_4
	(1)	(2) (3)	(4) (5)	(6) (7) (8)	(9)	(10)	(11)	(12) (13)
Natural HA[a] (R-9F)		2080, 1994	1454, 1427	1120, 999, –	964	875	–	614 –
Synthetic HA[b]		–	–	1092, 1065, 1028	962	–	633	603, 574 564
HA (this work) 1×10^5 Pa	3400	2078, 1994	1455, 1422	1110, 1090, 1050	962	875	633	603, 565
HA 4.3 GPa	3400	2079, 2000	1460, 1422	– 1091, 1037	961	876	632	602, 565
HA 8.5 GPa	3400	2077, 2002	1454, 1422	– 1091, 1034	960	875	632	602, 564
HA 10.5 GPa	3401	2080, 1992	1463, 1418	– 1090, 1033	960	875	632	602, 564

[a] Ref. [11]. Contains 0.13 wt % CO_2.
[b] Ref. [16].

spectrum. Based on this correlation, we estimate the carbonate content in our HA to be 0.6 wt %.

Data in Fig. 3 clearly show that the frequencies of the i.r. bands due to vibrational and librational modes of various functional groups do not show any significant change on application of pressure. However, the bands associated with phosphate groups exhibit pronounced narrowing at high pressures when the material transforms to an amorphous state (Fig. 1). Thus, the FWHM (full width at half maximum) of this band changes from 308 cm^{-1} for an unpressed sample to a new value of 278 and 220 cm^{-1} when the HA disc was subjected to 8.5 and 10.0 GPa pressure, respectively. This may be attributed to the rearrangement of the phosphate groups resulting in the weakening of their interaction with other lattice neighbours, a situation analogous to amorphization.

3.4. c → a transition

The substances such as SiO_2, GeO_2, $AlPO_4$, $LiKSO_4$ and some other compounds and minerals [23–27], which become amorphous at high pressures, have common network structures made up of corner-shared tetrahedra. The networks contain large interstitial voids, as in SiO_2 and in the tridymite like $LiKSO_4$ structure [26]. In some crystals the two types of structural units, such as AlO_4 and PO_4 tetrahedra in the crystal structure of $AlPO_4$ have different compressibilities. In such network structures, configurations with different relative orientation of co-ordination polyhedra have nearly the same free energy and compete with one another. The multiplicity of configurations, due to ease of polyhedral tilting, is known to facilitate the structural transformation on change of pressure and temperature [28]. The polyhedral tilt mechanism seems to be applicable to c → a transformation in HA also.

The structure of HA (space group $P6_3/m$) has six chains of PO_4 tetrahedra surrounding Ca_I atoms along the c-axis. The tetrahedra do not share the oxygen atoms among them, but are held between two pairs of Ca_I atom columns and two pairs of Ca_{II} atom columns along the c-axis (Fig. 4a). The Ca_I atoms, lying along the three-fold axis, are bonded to (6 + 3) oxygen atoms in six different PO_4 tetrahedra. The Ca_{II} atoms, situated along the hexagonal axis (6_3), each have seven-fold co-ordination with six oxygen atoms of five PO_4 tetrahedra and one OH ion [18]. The polyhedral model of the structure shows the oxygen atom lattice (Fig. 4b). The Ca_I and Ca_{II} atoms are at the centre of trigonal prisms and P atoms are at the centres of tetrahedra. The structure consists of columns of edge-shared trigonal prisms held together by loosely-stuffed columns of PO_4 tetrahedra. The cation

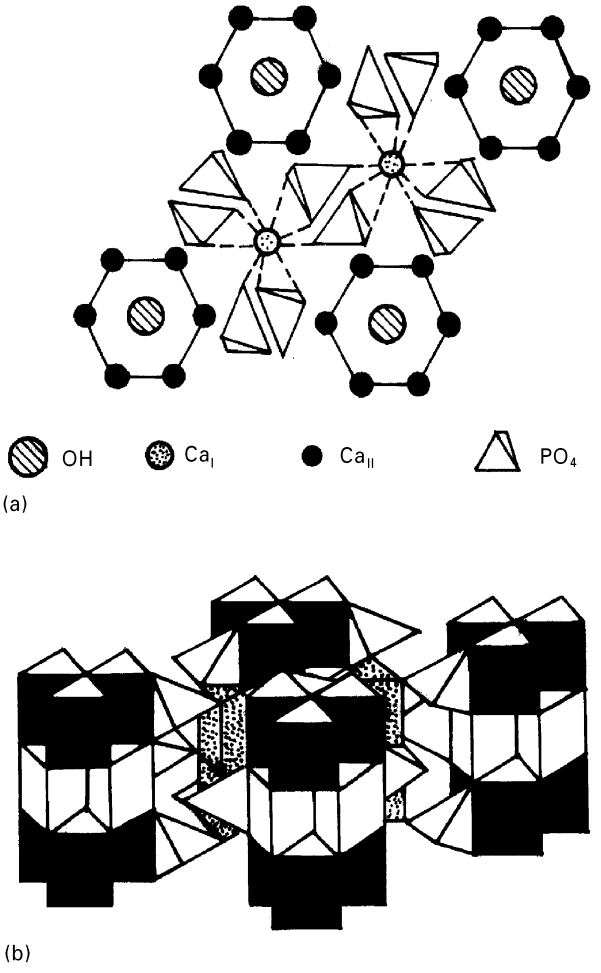

Figure 4 Crystal structure of hydroxylapatite. (a) Projection on the a–b plane; (b) polyhedral model of HA.

triangular prisms and PO_4 tetrahedra also have different compressibilities. The structure of HA is therefore susceptible to deformation under polyhedral tilt mechanism, and transition to amorphous phase sets in at about 2 GPa. The missing linkages between PO_4 groups perhaps make the HA structure more unstable than α-SiO_2, α-$AlPO_4$ and $LiKSO_4$ and consequently, amorphization pressure is also lower.

The pressure amorphized phases apparently result as a consequence of the equilibrium states being kinetically inaccesssible. In $Ca(OH)_2$, $LiKSO_4$ and $AlPO_4$, the pressure amorphized material reverts to a more stable crystalline phase upon decompression to zero pressure [25]. In contrast, $CaAl_2Si_2O_8$, Fe_2SiO_4 and calcium phosphates HA, α-TCP (tricalcium phosphate), DCPD (dicalcium phosphate dihydrate) and DCPA (dicalcium phosphate anhydrous) remain in metastable amorphous state after releasing pressure. In these materials, the crystalline order is destroyed by the inability of the structure to satisfy requisite bonding constraints due to kinetic factors. Thermodynamically and from a structural point of view, the amorphous phase may be regarded as an intermediate state of transition to a new ordered phase [27].

4. Conclusion

In the present study, using the techniques of XRD, SEM and FTIR, we have unequivocally established the occurrence of a pressure-induced crystalline to amorphous phase transformation in HA. Both the crystalline and the amorphous phases coexist at pressures in the range of 2 to 8.5 GPa, the relative concentration depending on the pressure. At pressures of 10.5 GPa and over, the material is found to be in near amorphous form.

Since the amorphous phase is likely to be more isotropic, we surmise that the HA powder subjected to intermediate pressures will serve as a composite material due to co-existing phases. Such materials may have better strength and binding and may prove useful for the medical applications. These aspects need further investigation.

References

1. M. JARCHO, C. H. BOLEN, M. B. THOMAS, J. BOBICK, J. F. KAY and R. H. DOREMUS, *J. Mater. Sci.* **11** (1976) 2027.
2. H. AOKI in "Science and medical application of hydroxylapatite" (Takayama Press, System Centre Co., 1991).
3. M. T. FULMER, R. I. MARTIN and P. W. BROWN, *J. Mater. Sci. Mater. Med.* **3** (1992) 299.
4. F. H. LIN, T. L. HARN and M. H. HON, *Ceram. Int.* **15** (1989) 351.
5. T. KIJIMA and M. TSUTSUMI, *J. Amer. Ceram. Soc.* **62** (1979) 455.
6. T. R. N. KUTTY, *Ind. J. Chem.* **11** (1973) 695.
7. M. AKAO, H. AOKI and K. KATO, *J. Mater. Sci.* **16** (1981) 809.
8. A. OSAKA, Y. MIURA, K. TAKEUCHI, M. ASADA and K. TAKAHASHI, *J. Mater. Sci. Mater. Med.* **2** (1991) 51.
9. R. I. MARTIN and P. W. BROWN, *ibid.* **6** (1995) 138.
10. S. PUAJINDANETR, S. M. BEST and W. BONFIELD, *Brit. Ceram. Trans.* **93** (1994) 96.
11. R. V. SANTOS and R. N. CLAYTON, *Amer. Mineral.* **80** (1995) 336.
12. A. BERTOLUZZA, S. CACCIARI, A. TINTI, M. VANISA and M. A. MORELLI, *J. Mater. Sci. Mater. Med.* **6** (1995) 76.
13. M. J. LeBAS, C. D. HANDLEY, *Nature* **279** (1979) 54.
14. G. H. McCELLEN and J. R. LEHR, *Amer. Mineral.* **54** (1969) 1374.
15. V. C. FARMER (ed.) "The infrared spectra of minerals" (Mineralogical Society, London, 1974) Monograph no. 4 p. 227.
16. C. B. BADDIEL and E. E. BERRY, *Spectrochim. Acta* **22** 1996 1407.
17. JCPDS Data File – Card No. 9–432.
18. A. S. POSNER, A. PERLOFF and A. F. DIORIO, *Acta Crystallogr.* **11** (1958) 308.
19. V. VIJAYAKUMAR, S. N. VAIDYA, E. V. SAMPATHKUMARAN and L. C. GUPTA, *High. Temp – High Press.* **12** (1980) 649.
20. S. N. VAIDYA, D. K. JOSHI and C. KARUNAKARAN, *Ind. J. Technol.* **14** (1976) 679.
21. A. V. MILOVSKY and O. V. KONONOV, "Mineralogy", (Mir Publishers, Moscow, 1985) p. 235.
22. K. J. KINGMA, R. J. HEMLEY, H. K. MAO and D. R. VEBLEN, *Phys. Rev. Lett.* **70** (1993) 3927.
23. R. J. HEMLEY, A. P. JEPHCOAT, H. K. MAO, L. C. MING and M. H. MANGHANANI, *Nature* **334** (1988) 52.
24. M. MADON, Ph. GILLET, Ch. JULIEN and G. D. PRICE, *Phys. Chem. Min.* **18** (1991) 7.
25. M. B. KRUGER and R. JEANLOZ, *Science* **249** (1990) 647.
26. H. SANKARAN, S. K. SIKKA, S. M. SHARMA and R. CHIDAMBARAM, *Phys. Rev.* B **38** (1988) 170.
27. S. K. SIKKA and S. M. SHARMA, *Curr. Sci.* **63** (1992) 317.
28. R. M. HAZEN and W. FINGER, *Phase Transitions* **1** (1979) 1.

Received 25 March 1996
and accepted 9 January 1997